ROYAL SOCIETY OF CHEMISTRY

Journal Name

ARTICLE

Unexpected formation of a fused double cycle trinuclear gold(I) complex supported by *ortho*-phenyl metallated aryl-diphosphine ligands and strong aurophilic interactions

Csaba Jobbágy,[a] Péter Baranyai,[a] Pál Szabó,[b] Tamás Holczbauer,[c] Barbara Rácz,[a] Liang Li,[d] Pance Naumov*[d] and Andrea Deák*[a]

The first homoleptic trinuclear arylgold(I) complex, [Au$_3$(L')$_2$](NO$_3$) (**3**), based on *ortho*-phenyl metallated aryl-diphosphine ligand (L' = *o*-C$_6$H$_4$PPh(C$_{15}$H$_{10}$O)PPh$_2$), has been obtained through a new thermolytic reaction of the corresponding diauracycle, [Au$_2$(L)$_2$](NO$_3$)$_2$ (L = xantphos). The formation of **3** involves the activation of the *ortho*-phenyl C–H bond of the xantphos ligands. The presence of the Au–C bonds in this new gold-diphosphine cluster is not its only remarkable feature, since it also displays two 12-membered rings fused together and a linear {Au$_3$} chain with aurophilic interactions. Complex **3** exhibits strong sky-blue luminescence that can be assigned to triplet metal-metal (^{3}MM) transition partially mixed with ligand-to-metal-metal charge transfer (^{3}LMMCT) transition related to the aurophilic bonding. This [Au$_3$(L')$_2$]$^+$ triauracycle also shows AIEE-activity, and is a selective luminescent chemosensor for metal ions.

Introduction

In general, synthetic chemists aim to create new materials through chemical transformations where chemical bonds being made or broken. Some of the as-obtained new compounds often have unusual structures and intriguing properties. Among metal-based compounds, gold(I) derivatives with polyphosphine ligands containing gold–phosphorous bonds are endowed with unconventional structural features and chemical functionalities.[1–5] Gold(I) derivatives are also attracting interest as functional new materials due to their exciting potential applications in mechano- and chemosensors, data recording, nanochemistry and catalysis.[1] Yet, the main inspiration to study these structures comes from their superb emission properties related to aurophilic interactions.[6] One of the strategies to elicit luminescence by Au···Au contacts relies upon the use of polyphosphines as connecting units to generate homoleptic rings.[2,3] This approach affords homoleptic di-, tri- and tetranuclear gold(I) complexes containing only bridging polyphosphine ligands and short Au···Au contacts.[2,3] The possibility of external control of the luminescent properties of some of these structures by multiple external stimuli,[3] adds a new and important direction to this research.

Recently, we reported that 16-membered diauracycles based on diphosphine (diphos) ligands, [Au$_2$(diphos)$_2$](X)$_2$, can alter their luminescence in response to physical and chemical stimuli.[3] Combining diphosphines with other bridging ligands such as diacetylides or diisocyanides results in a great diversity of larger heteroleptic dialkynylgold(I) rings featuring gold–carbon bonds.[4] The presence of alkynylgold(I) units enhances the photoluminescent properties of these heteroleptic gold(I) macrocycles.[4] Although examples of homoleptic and heteroleptic rings containing gold(I) centers are known, preparation of cyclic aryl- or alkylgold(I) complexes based exclusively on bridging polyphosphine ligands remains a challenge. The only known example, a pentanuclear gold cluster that contains a methylene monoaurated diphosphine ligand,[5] was prepared by gold evaporation.[7] Along this line of pursuit, herein we present the first homoleptic trinuclear arylgold(I) complex that features two *ortho*-phenyl metallated diphosphine ligand and shows striking emission properties both in solution and in solid state. Although some large 16- and 21-membered macrocycles containing three gold(I) centres and only diphosphine ligands have been reported,[8] this triauracycle complements these examples with a metallacycle that consists of two 12-membered rings fused together having a linear {Au$_3$} chain with short Au···Au contacts and Au–C bonds. In this communication, we also report the thermally-induced mechanical effect of crystals of the precursor diphosphine-based diauracycle that lead to the discovery of this arylcyclometallated gold(I) complex. This is the first report on aggregation-induced enhancement emission and metal ion chemosensing luminescent properties from a diphosphine-based arylgold(I) system.

a. *Hungarian Academy of Sciences, MTA TTK SZKI, "Lendület" Supramolecular Chemistry Research Group, 1117 Budapest, Magyar Tudósok körútja 2, Hungary; E-mail: deak.andrea@ttk.mta.hu*

b. *Hungarian Academy of Sciences, MTA TTK SZKI, MS Metabolomics Research Group, 1117 Budapest, Magyar Tudósok körútja 2, Hungary;*

c. *Hungarian Academy of Sciences, MTA TTK SZKI, Chemical Crystallography Research Group, 1117 Budapest, Magyar Tudósok körútja 2, Hungary;*

d. *New York University Abu Dhabi, P.O. Box 129188, Abu Dhabi, United Arab Emirates; Email: E-mail: pance.naumov@nyu.edu*

Results and discussion

Our previous studies have shown that the dinuclear gold(I) complex of the ligand xantphos (L = 9,9-dimethyl-4,5-bis(diphenylphosphino)-xanthene, $Ph_2P(C_{15}H_{10}O)PPh_2$), $[Au_2(L)_2](NO_3)_2 \cdot 2.64\ CH_2Cl_2$ (**1**) changes its blue emission into orange-red in response to mechanical stimuli.[3a] When heated from room temperature to 220 °C, crystals of **1** exhibit a visually impressive mechanical effect—they hop off the stage (Movie S1), in a manner that resembles the thermosalient effect.[9] Intrigued by this observation, we investigated the products of the thermal decomposition of the crystals of **1**. As shown in Figure 1, bubbles evolve from a crystal which has been immersed in silicone oil and heated up to 250 °C as a result of the gas that emanates from the crystal (Movie S2). Pyrolysis gas chromatography–mass spectrometry (Py GC–MS) showed release of the solvent (CH_2Cl_2) and NO (Figure S4). Thus, unlike the thermosalient effect which is due to a phase transition, the mechanical effect of the crystals of **1** is due to release of gas, similar to what has been observed with crystals of nitronyl nitroxide metal complexes.[9b]
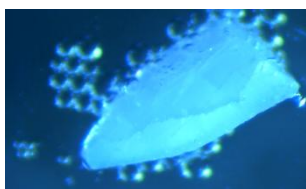
Figure 1. Optical microscopy image of crystal **1** in 250 °C silicone oil.

The brownish thermolysate of **1** was dissolved in CH_2Cl_2 and analysed by electrospray mass spectrometry (ESI-MS). Normal MS and tandem (MS/MS) spectra (Figures S6–S14) were recorded in order to identify the structures of species formed. A representative ESI-MS spectrum (Figure S6) shows the dissociation of dinuclear $[Au_2(L)_2]^{2+}$ cations into mononuclear $[Au(L)]^+$ species (*m/z* 775). Oxidation products such as xantphos dioxide $[LO_2 + 1H]^+$ (*m/z* 611), as well as gold(I) xantphos oxide (LO) species, $[Au(LO)]^+$ (*m/z* 791) and $[Au(LO)_2]^+$ (*m/z* 1385), were also observed. The other characteristic peaks at *m/z* 1007, 1565 and 1745 belong to gold(I) xantphos species (see the discussion below).

It appears that the thermolysis of **1** proceeds through a redox reaction that results in nitrate reduction to NO, oxidation of the xantphos and formation of complex mixture of products including several gold(I) species of xantphos and xantphos oxide. Some more insight into the process of thermolysis was obtained during the attempts to recrystallize the brownish thermolysate of **1**. Efforts to obtain single crystals were only successful when the thermolysate of **1** was washed with toluene, and the remaining brownish solid was dissolved in a mixture of dichloromethane and toluene. Slow evaporation of this mixture at 50 °C produced colourless crystals of **2** and yellow crystals of **3** (Figure S1). The thermolysis of **1** followed by washing with toluene and recrystallization from dichloromethane–toluene mixture has been summarized in Scheme 1.
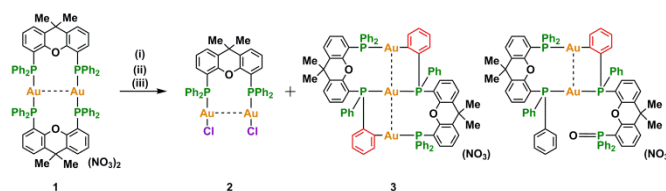
Scheme 1. Thermolysis of **1** followed by recrystallization based on the structure of the products. Conditions: (i) heating at 180 °C, (ii) washing with toluene and (iii) recrystallization from dichloromethane-toluene mixture.

Single crystal X-ray diffraction analysis of the colourless crystals of **2** showed that these are either the dichloromethane or the toluene solvates of the dinuclear complex $Au_2(L)Cl_2$ (**2**). The structure of the dichloromethane solvate was previously reported.[6a] In the toluene:dichloromethane (0.8:0.2) solvate **2**, the phosphorous atoms of the xantphos ligand bridge the gold(I) centres, and the distance between them is 2.968(1) Å (Figure 2). This intramolecular aurophilic interaction, as well as the bond distances Au–P [2.235(2) Å] and Au–Cl [2.313(2) and 2.295(2) Å] are similar to those found in the dichloromethane solvate. The gold centres approach a linear P–Au–Cl geometry, and the corresponding bond angles are 169.9(1) and 173.7(1)°, respectively. The torsion angles P–Au–Au–P and Cl–Au–Au–Cl [80.6(1)° and 82.2(1)°] are smaller than those found in dichloromethane solvate [87.1(1)° and 90.7(1)°]. The dinuclear molecules of **2** form C–H···Cl bonded dimers in the crystal of the toluene solvate.
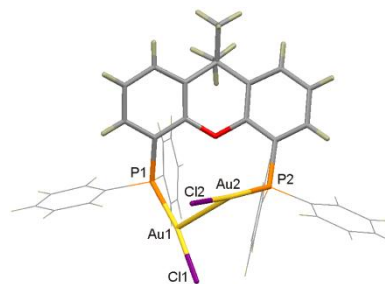
Figure 2. Molecular structure of **2**. Colour scheme: gold, yellow; phosphorous, orange; carbon, grey; oxygen, red; chlorine, purple; hydrogen, dark brown. The phenyl groups are shown as a wireframe model. The solvate molecules are omitted for clarity.

This formation of **2** must involve C–Cl bond activation of CH_2Cl_2 molecules. Dinuclear $[Au_2(L)(Cl)]^+$ species derived upon C–Cl bond cleavage of dichloromethane were observed in the ESI MS spectrum at *m/z* 1007 (Figure S6). While a variety of dinuclear gold(II) and mononuclear gold(III) compounds were prepared by gold(I)-mediated oxidative addition of dichloromethane,[10,11] this is a rare observation of formation of a gold(I) halide complex by activation of the C–Cl bond in CH_2Cl_2. Schmidbaur and Fackler studied extensively the oxidative addition of dihalomethanes CH_2X_2, halogens X_2 (X = Cl, Br and I) and alkyl halides to eight-membered dinuclear gold(I) ylide complexes, $[Au_2(CH_2PR_2CH_2)]_2$.[11] These reactions occur with one-electron oxidation at each gold centre and shortening of the Au(II)···Au(II) distance.[11] However, it was also shown that the $[Au_2(diphos)_2]^{2+}$ complexes can not oxidatively add small molecules or easily oxidize.[11e,12a] Thus, no oxidative addition of halogens occurred for eight-membered $[Au_2(dppm)_2]^{2+}$ (dppm =

Ph$_2$PCH$_2$PPh$_2$) complex.[12a] In the resulting products, such as [Au$_2$(dppm)$_2$(Br)$_2$], the bromide ions are coordinated to gold centres, whereas in [Au$_2$(dppm)$_2$(μ-I)](I), one iodide bridges the gold centres and the other one is non-coordinated.[12a] Moreover, it was also reported that the eight-membered dinuclear [Au$_2$(dcpm)$_2$]$^{2+}$ complex based on bis(dicyclohexylphosphine)methane (dcpm) is an effective photocatalyst for UV-induced C–Cl bond cleavage of CH$_2$Cl$_2$. The photolysis (irradiation with λ > 260 nm) results in formation of Au$_2$(dcpm)(Cl)$_2$ however the mechanism of photoconversion is complex and requires further studies.[12b] In our case, as suggested by the Py GC–MS and ESI-MS data, the nitrate reduction to NO is accompanied by the oxidation of xantphos (L) to xantphos dioxide (LO$_2$). The formation of LO$_2$ must lead to Au–P bond cleavage and ring opening of **1**, which would leave the Au(I) centres coordinatively unsaturated. We propose that the as-formed [Au$_2$L]$^{2+}$ cationic intermediate abstracts Cl$^-$ anion from CH$_2$Cl$_2$ to form neutral Au$_2$(L)Cl$_2$ (**2**). However, the mechanism regarding the activation of C–Cl bond and formation of **2** is far from understood and further studies are needed.
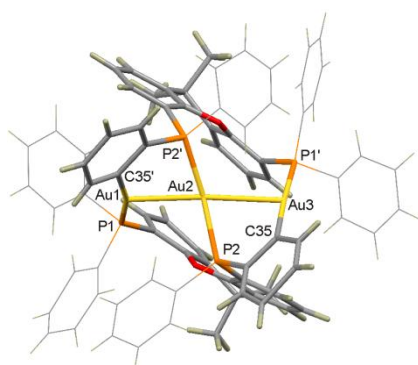

Figure 3. Molecular structure of [Au$_3$(L')$_2$]$^+$ cation in **3**. Colour scheme: gold, yellow; phosphorous, orange; carbon, grey; oxygen, red; hydrogen, dark brown. The phenyl groups are shown as a wireframe model. Only the major disorder component is shown.

As shown in Figure S2, the yellow crystals of **3** show intense bright blue emission when irradiated at 365 nm with UV lamp. Despite weak X-ray scattering due to a combination of weak crystallinity, solvation and disorder (see details in SI), the crystal structure of the yellow crystal of **3** revealed that it consists of cycloaurated [Au$_3$(L')$_2$]$^+$ and [Au$_2$(L')(LO)]$^+$ cations (L' = o-C$_6$H$_4$PPh(C$_{15}$H$_{10}$O)PPh$_2$), in an approximate 60:40 ratio, NO$_3^-$ anions and toluene solvent molecules. It should be noted that the ESI-MS spectrum of brownish termolysate of **1** (Figure S6) showed a peak at m/z 1565 and 1745, characteristic to monovalent [Au$_2$(L')(LO)]$^+$ and [Au$_3$(L')$_2$]$^+$ cation. The trinuclear cycloaurated [Au$_3$(L')$_2$]$^+$ cation depicted in Figure 3, with the disorder omitted for clarity. This [Au$_3$(L')$_2$]$^+$ cation features two $ortho$-phenyl aurated xantphos (L') ligands, each of which is P,P,C-coordinated to three gold(I) atoms. This cation displays an unprecedented coordination mode of the xantphos ligand, and the $ortho$-phenyl auration of a diphosphine ligand has never been observed before. There are two different gold(I) centres in this biaryl gold(I) cation: Au(1) and Au(3) are bonded to the phosphorous and carbon atoms, whereas Au(2) is bonded to phosphorous atoms of the L' ligands. The Au–P bond lengths are

comparable to those found in gold(I) complexes with xantphos.[3] The Au–C σ-bond lengths [2.18(1) and 2.21(2) Å] are similar to those reported in arylgold(I) complexes.[13] The P–Au–C angles are 164.0(5) and 174.7(3)°, whereas the P–Au–P angle is 161.2(2)°. The P–Au–Au–P torsion angles, which are 67.2(2) and 71.0(2)° respectively, suggest that the $ortho$-phenyl aurated xantphos ligands of **3** are more folded than the xantphos ligand in **2**. To our knowledge, **3** represents the first structurally characterized arylcyclometallated gold(I) complex with bridging anionic diphosphine ligand. Based on structure of **3**, it is also worth mentioning that only a few instances of gold(I)-mediated C–H activation of arenes has been reported yet.[14] Direct C–H auration with Au(I) compounds specific for electron-poor arenes is believed to proceed via concerted metalation-deprotonation or deprotonation-metalation mechanisms.[14] Larossa reported that the strong π-coordination ability of ^{t}Bu$_3$PAuCl to arenes lead to direct C–H activation via σ-bond metathesis and HCl elimination.[14a] In our case, it should be expected that an interconversion between Au$_2$(L)(Cl)$_2$ and [Au(L)]$^+$ species, both present in the thermolysate, could lead to the formation of a trinuclear [Au$_3$(L)$_2$(Cl)$_2$]$^+$ intermediate, as observed in the ESI-MS/MS spectrum (Figure S14). While detailed mechanistic data are thus far not at hand, we hypothesize that concerted intramolecular $ortho$-metalation of the pendant aryl ring of L of the [Au$_3$(L)$_2$(Cl)$_2$]$^+$ cation followed by HCl elimination leading to Au–C bond formation could be a viable route to the formation of cyclic [Au$_3$(L')$_2$]$^+$ cation. It is not yet clear how [Au$_3$(L')$_2$]$^+$ was formed, since the mixture was not protected from light a radical mechanism cannot be ruled out. Moreover, it cannot be ruled out the presence of catalytic amounts of Au(III) species formed upon oxidative addition of CH$_2$Cl$_2$, which would also facilitate the C–H bond activation of pendant aryl ring of the L ligand.
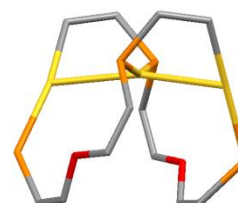

Figure 4. Two 12-membered Au$_2$P$_3$C$_6$O$_1$ rings fused together, having a {Au$_3$} chain in **3**. Colour scheme: gold, yellow; phosphorous, orange; carbon, grey; oxygen, red.

As shown in Figure 4, the [Au$_3$(L')$_2$]$^+$ cation consists of two 12-membered Au$_2$P$_3$C$_6$O$_1$ rings fused together (Figure 4). These topologically interesting 12-membered rings assume a twisted conformation, whereas the gold atoms form an almost linear {Au$_3$} chain (Au···Au···Au angle is 166.9(1)°), with intramolecular Au···Au contacts of 2.783(2) and 2.850(1) Å, respectively. Linear {Au$_3$} chains have been found in 12-membered trigold(I) complexes of bridging triphosphine ligands.[2b] Previously, a 16-membered macrocycle containing a {Au$_3$} triangle has been prepared by employing pyridyl-2,6-diphenyl^{2-} and bridging diphosphine ligand.[15] Laguna reported some polynuclear gold complexes with linear {Au$_n$} chains (n = 3, 5 and 6), wherein the gold atoms are in different oxidation states.[16] For example, the backbone of the tetranuclear [Au$_4$(C$_6$F$_5$)$_2${(Ph$_2$P)$_2$CH}$_2$(Ph$_3$P)$_2$]

complex is a linear {Au$_3$} chain of four-coordinated gold atoms, which feature either Au^{II}···Au^{I}···Au^{II} or Au^{I}···Au^{III}···Au^{I} oxidation states.[16a] Within this linear {Au$_3$} chain the intramolecular Au···Au contacts are 2.731(2) and 2.909(2) Å, respectively. Among large macrocycles containing three gold(I) centres and only diphosphine ligands,[8] our macrocycle represents the first trigold(I) macrocycle that features a linear {Au$_3$} chain with short Au···Au contacts. Further examination of the crystal structure of **3** revealed that there are C–H···O interactions between the [Au$_3$(L')$_2$]$^+$ cations and NO$_3^-$ anions.

The absorption spectrum of **3** in CH$_2$Cl$_2$ shows two intense bands in the UV region (Figure 5a). On the basis of DFT calculations (see details in SI) on the optimized singlet ground state structure of [Au$_3$(L')$_2$]$^+$ cation and TDDFT analysis, the lowest energy absorption band (λ = 356 nm) is assigned to the transition between the highest occupied molecular orbital and the lowest unoccupied molecular orbital (HOMO → LUMO, λ_{calc} = 326 nm, f (oscillator strength) = 0.193; Figure S24, Table S4). The HOMO is predominantly metal sdσ* character and LUMO has its major contribution coming from the gold pσ orbitals and phosphine ligands. Therefore the HOMO → LUMO transition tentatively attributed to the metal-metal-to-ligand-charge-transfer (MMLCT) transition (Table S5). The absorption band at 292 nm is assigned to the HOMO − 2 → LUMO + 2 transition (λ_{calc} = 272 nm, f = 0.154; Figure S24, Table S4), which can be described as π → π* transition within the xanthphos ligand (Table S5).
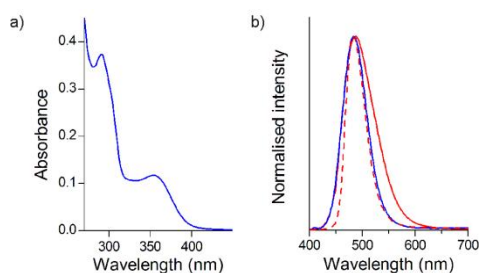

Figure 5. a) UV/VIS absorption spectra of **3** in CH$_2$Cl$_2$ (10 μM) and b) its emission spectra in CH$_2$Cl$_2$ solution (solid blue line) and in solid state at room temperature (solid red line) and at 77 K (dashed red line) upon excitation with 365 nm.

Complex **1** is not luminescent in solution due to the conformational flexibility of the [Au$_2$(L)$_2$]$^{2+}$ cation that opens nonradiative deexcitation channels.[3] To attain luminescence in solution it is necessary to avoid these pathways by sterically hindering the conformational changes. The linear Au$_3$ chain of aurophilic interactions and the tridentate μ-bridging of the xanthphos ligands confer enhanced structural rigidity to cycloaurated [Au$_3$(L')$_2$]$^+$ cations relative to the conformationally flexible dinuclear species [Au$_2$(L)$_2$]$^{2+}$. The HRMS-ESI spectrum (Figure S3) shows a prominent cluster peak at *m/z* 1745 and confirm the existence of trinuclear [Au$_3$(L')$_2$]$^+$ cations in dichloromethane solution. **3** becomes weakly emissive at room temperature in deoxygenated CH$_2$Cl$_2$ or MeOH solution with a maximum emission at 480 nm (Figure 5b) which exhibits single-exponential behaviour with a lifetime of 180 ns. The emission intensifies when water, an anti-solvent of **3**, is added (Figure 6a). The emission of **3** in methanol is strongly enhanced

between 60 and 80 vol% water (Figure 6b) and in a methanol-water mixture with 80% of water the luminescence intensity is 20 times that in pure methanol (Figure 6c). Moreover, we observed that the emission intensity in a methanol-water mixture with 99% of water is lower than that with 90% water. These results indicate that the intramolecular dynamics of the molecules is restricted and the emission of **3** is enhanced by formation of aggregates. Thus, **3** shows aggregation-induced emission enhancement (AIEE) activity.[17]
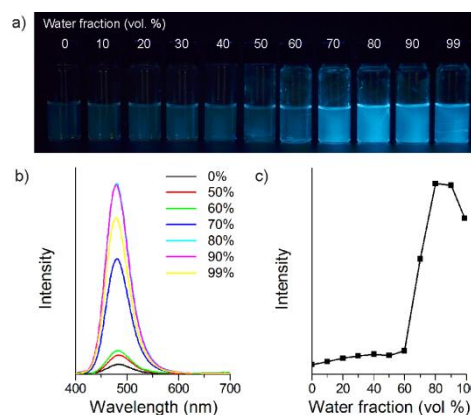

Figure 6. a) Photographs of **3** in methanol-water mixtures (0–99 vol. %) with different water fractions taken under 365 nm illumination; b) Emission spectra of **3** in methanol-water mixtures with different water fractions and c) Luminescence intensity of **3** at 480 nm versus the composition methanol-water mixtures (0–99 vol. %).

3 is strongly emissive and emits light with bright blue colour in the solid state at room temperature with maximum at 480 nm, which is red shifted by 4 nm at 77 K. The very small difference between the emission maxima measured in different phases and the small temperature effect might reflect the structural rigidity of [Au$_3$(L')$_2$]$^+$ cations. The decay of luminescence in the solid state can be described with a monoexponentional function with lifetimes of 0.9 and 1.8 μs at 298 and 77 K, respectively. The large Stokes shift and the microsecond lifetimes indicate that the emission originates from a triplet state.[6a]
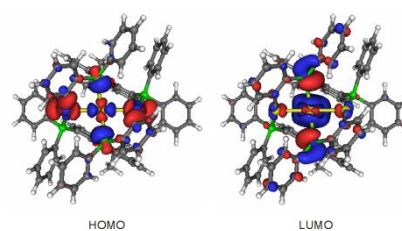

Figure 7. Contour plots of the HOMO and LUMO superimposed on the excited triplet (T$_1$) state geometry of [Au$_3$(L')$_2$]$^+$.

To elucidate the luminescence properties of **3**, we performed quantum chemical calculations on the lowest excited triplet state (T$_1$) of [Au$_3$(L')$_2$]$^+$ cation by DFT and TD DFT methods (see SI for details). The structure for the lowest excited triplet state (T$_1$) was optimized with the hybrid UPBE0[18] functional using the LANL2DZ effective core potential for the Au centres and the standard 6-31G* basis set for the remaining atoms. In the optimized geometry of T$_1$ excited state the Au···Au distances are reduced by more than 0.3 Å with increase of the Au···Au···Au

angle to 177.7°, showing a light induced contraction and linearization of the {Au$_3$} chain (Table S3). According to TD DFT calculation the phosphorescence from T$_1$ state could be described almost exclusively (orbital contribution: 98%, Table S4) as transition between LUMO and HOMO (Figure 7). The calculated T$_1 \rightarrow$ S$_0$ emission wavelength (583 nm) for [Au$_3$(L')$_2$]$^+$ cation predicted by TD DFT method was greatly overestimated, however the energy difference between the highest singly occupied molecular orbital (H-SOMO) and lowest singly occupied molecular orbital (L-SOMO) at the optimized T$_1$ geometry provides an emission maximum at 459 nm,[18c] which is in good agreement with the experimental value measured for blue luminescence of **3**. The TD DFT and molecular orbital analysis show that the HOMO and LUMO concentrate mainly on gold atoms and the contribution of phosphine ligands to the electron density is smaller in case of HOMO (Figure 7, Table S5). Thus, according to theoretical calculations the emission can be assigned as arising from triplet metal centred (^{3}MM) transition mixed with ligand-to-metal-metal charge transfer (^{3}LMMCT) transition related to the presence of aurophilic bonding.

We tested the luminescence response of **3** to metal ions, such as Cu^{2+}, Ag$^+$, Hg^{2+}, Co^{2+}, Ni^{2+} and Zn^{2+}. Air-dried filter paper strips impregnated with a solution of **3** in dichloromethane were treated with few drops of solutions of metal ions. As shown in Figure 8a, the emission was almost unaffected by Ni^{2+} and Zn^{2+}. On the other hand, metal ions such as Co^{2+} and Cu^{2+} significantly quenched the emission, and with Hg^{2+} the luminescence was completely quenched. The colour change in presence of Ag$^+$ ions is particularly striking—upon addition of metal ions the sky-blue luminescence changes into strong greenish-yellow emission (Figure 8a). This visually distinguishable luminescent behaviour of **3** in the presence of Ag$^+$ ions favours this compound as a sensitive and selective luminescence sensor for Ag$^+$ ions.
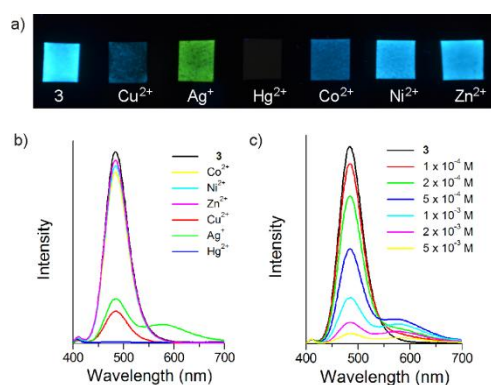

Figure 8. a) Photographs taken under 365 nm UV illumination showing the effect of different metal ions on the luminescence of **3**; b) Emission spectra of **3** in methanol (10 μM) with different metal cations at concentration of 10^{-3} M and c) Emission spectra of **3** in the presence of increasing concentration of Ag$^+$.

A methanol solution of **3** (1 × 10^{-5} M) is weakly emissive in the absence of metal ions. The luminescence spectrum of **3** in the presence of different metal cations, including Cu^{2+}, Ag$^+$, Hg^{2+}, Co^{2+}, Ni^{2+} and Zn^{2+} at a concentration of 10^{-3} M, is shown in Figure 8b. Ni^{2+}, Zn^{2+} and Co^{2+} had little influence on the emission intensity (Figure 8b) contrarily Cu^{2+} cation showed strong

quenching effect. In case of Hg^{2+} cation the quenching of the blue luminescence was delayed, namely the emission completely disappeared after 15 minutes. The addition of Ag$^+$ to **3** in methanol caused the appearance of a new emission band at 577 nm in parallel with an intensity decreasing at 480 nm, whereas at higher concentration of metal ion both emission bands were gradually quenched (Figure 8c).

Conclusions

In summary, a homoleptic trinuclear arylgold(I) complex (**3**) featuring two *ortho*-phenyl aurated diphosphine ligands is reported here that was obtained through a new thermolytic reaction of a diphosphine-based diauracycle (**1**), followed by recrystallization. The as-obtained triauracycle features two 12-membered rings fused together, which contains a linear {Au$_3$} chain that shows strong room-temperature luminescence. To our knowledge, arylcyclometallated Au(I) complexes with bridging anionic diphosphine ligands have not been reported yet. The formation of **2** and **3** involves activation of the C–Cl bond of dichloromethane and activation of the aryl C–H bond of the diphosphine ligands. These C–H and C–Cl bond activations could be applicable to other relevant gold(I)-catalyzed chemical processes. Thorough studies on the mechanism and the exact role of Au(I) in these transformations are now underway in our laboratory.

Acknowledgments

References

1 (*a*) S. L. James, *Chem. Soc. Rev.*, 2009, **38**, 1744–1758; (*b*) M. J. Irwin, L. M. Rendina, J. J. Vittal and R. J. Puddephatt, *Chem. Commun.*, 1996, 1281–1282; (*c*) R. J. Puddephatt, *Coord. Chem. Rev.* 2001, **216–217**, 313–332; (*d*) Cs. Jobbágy, A. Deák, *Eur. J. Inorg. Chem.* 2014, 4434–4449.

2 (*a*) V. W.-W. Yam, T.-F. Lai and C.-M. Che, *Dalton Trans.*, 1990, 3747–3752; (*b*) W. Schuh, H. Kopacka, K. Wurst and P. Peringer, *Chem. Commun.*, 2001, 2186–2187; (*c*) M.-C. Brandys and R. J. Puddephatt, *Chem. Commun.*, 2001, 1280–1281; (*d*) W.-F. Fu, K.-C. Chan, V. M. Miskowski and C.-M. Che, *Angew. Chem. Int. Ed.*, 1999, **38**, 2783–2785; (*e*) W.-F. Fu, K.-C. Chan, K.-K. Cheung and C.-M. Che, *Chem. Eur. J.*, 2001, **7**, 4656–4664; (*f*) (*g*) (*h*) M. Bardají, A. Laguna, V. M. Orera and M. D. Villacampa, *Inorg. Chem.*, 1998, **37**, 5125–5130; (*i*) G. S. M. Tong, S. C. F. Kui, H.-Y. Chao, N. Zhu and C.-M. Che, *Chem. Eur. J.*, 2009, **15**, 10777–10789; (*j*) Y. Takemura, H. Takenaka, T. Nakajima and T. Tanase, *Angew. Chem. Int. Ed.*, 2009, **48**, 2157–2161.

3 (*a*) A. Deák, T. Megyes, G. Tárkányi, P. Király, L. Biczók, G. Pálinkás and P. J. Stang, *J. Am. Chem. Soc.*, 2006, **128**, 12668–12670; (*b*) T. Tunyogi, A. Deák, G. Tárkányi, P. Király and G. Pálinkás, *Inorg. Chem.*, 2008, **47**, 2049–2055; (*c*) A. Deák, T. Tunyogi, Z. Károly, Sz. Klébert and G. Pálinkás, *J. Am. Chem.*

Soc., 2010, **132**, 13627–13629; (*d*) Cs. Jobbágy, M. Molnár, P. Baranyai, A. Hamza, G. Pálinkás and A. Deák, *CrystEngComm*, 2014, **16**, 3192–3202; (*e*) Cs. Jobbágy, M. Molnár, P. Baranyai and A. Deák, *Dalton Trans.*, 2014, **43**, 11807–11810; (*f*) A. Deák, Cs. Jobbágy, G. Marsi, M. Molnár, Z. Szakács and P. Baranyai, *Chem. Eur. J.*, 2015, **21**, 11495–11508; (*g*) P. Baranyai, G. Marsi, Cs. Jobbágy, A. Domján, L. Oláh and A. Deák, *Dalton Trans.*, 2015, **44**, 13455–13459;

4   (*a*) C. P. McArdle, M. J. Irwin, M. C. Jennings, J. J. Vittal and R. J. Puddephatt, *Chem. Eur. J.*, 2002, **8**, 723–734; (*b*) W. J. Hunks, J. Lapierre, H. A. Jenkins and R. J. Puddephatt, *Dalton Trans.*, 2002, 2885–2889; (*c*) W. J. Hunks, M.-A. MacDonald, M. C. Jennings and R. J. Puddephatt, *Organomet.*, 2000, **19**, 5063–5070; (*d*) V. W.-W. Yam, S. W.-K. Choi and K.-K. Cheung, *Organomet.*, 1996, **15**, 1734–1739.

5   J. W. A. van der Velden, J. J. Bour, F. A. Vollenbroek, P. T. Beurkens and J. M. M. Smits, *Chem. Commun.*, 1979, 1162–1163.

6   (*a*) A. Pintado-Alba, H. de la Riva, M. Nieuwhuyzen, D. Bautista, P. R. Raithby, H. A. Sparkes, S. J. Teat, J. M. López-de-Luzuriaga and M. C. Lagunas, *Dalton Trans.*, 2004, 3459–3467; (*b*) M. A. Rawashdeh-Omary, J. M. López-de-Luziriaga, M. D. Rashdan, O. Elbjeirami, M. Monge, M. Rodríguez-Castillo and A. Laguna, *J. Am. Chem. Soc.*, 2009, **131**, 3824–3825; (*c*) H. Ito, M. Muromoto, S. Kurenuma, S. Ishizaka, N. Kitamara, H. Sato and T. Seki, *Nat. Commun.*, 2013, **4**, 2009; (*d*) T. Seki, K. Sukurada and H. Ito, *Angew. Chem. Int. Ed.*, 2013, **52**, 12828–12832.

7   F. A. Vollenbroek, P. C. P. Bouten, J. M. Trooster, J. P. van den Berg and J. J. Bour, *Inorg. Chem.*, 1978, **5**, 1345–1347.

8   (*a*) S. Bhargava, K. Kitadai, T. Masashi, D. W. Drumm, S. P. Russo, V. W.-W. Yam, T. K.-M. Lee, J. Wagler and N. Mirzadeh, *Dalton Trans.*, 2012, **41**, 4789–4798; (*b*) J. H. K. Yip and J. Prabhavathy, *Angew. Chem. Int. Ed.*, 2001, **40**, 2159–2162.

9   (*a*) P. Naumov, S. Chizhik, M. K. Panda, N. K. Nath and E. Boldyreva, *Chem. Rev.*, 2015, **115**, 12440–12490; (*b*) V. I. Ovcharenko, S. V. Fokin, E. Y. Fursova, O. V. Kuznetsova, E. V. Tretyakov, G. V. Romanenko and A. S. Bogomyakov, *Inorg. Chem.*, 2011, **50**, 4307–4312.

10 D. Aguilar, M. Contel and E. P. Urriolabeitia, *Chem. Eur. J.*, 2010, **16**, 9287–9296.

11 (*a*) P. Jandik, U. Schubert and H. Schmidbaur, *Angew. Chem. Int. Ed.*, 1982, **21**, 73; (*b*) H. Schmidbaur and P. Jandik, *Inorg. Chim. Acta*, 1983, **74**, 97–99; (*c*) J. P. Fackler and J. D. Basil, *Organomet.*, 1982, **1**, 871–873; (d) H. H. Murray, J. P. Fackler and A. M. Mazany, *Organomet.*, 1984, **3**, 1310–1311; (*e*) J. P. Fackler, *Polyhedron*, 1997, **16**, 1–17; (*f*) A. Laguna and M. Laguna, *Coord. Chem. Rev.*, 1999, **193**–**195**, 837–856.

12 (*a*) J. Shain and J. P. Fackler, *Inorg. Chim. Acta*, 1987, **131**, 157–158; (*b*) C. Ma, C. T.-L. Chan, W.-P. To, W.-M. Kwok and C.-M. Che, *Chem. Eur. J.*, 2015, **21**, 13888–13893.

13 (*a*) D. V. Partyka, J. B. Updegraff III, M. Zeller, A. D. Hunter and T. G. Gray, *Organomet.*, 2009, **28**, 1666–1674; (*b*) C. Croix, A. Balland-Longeau, H. Allouchi, M. Giorgi, A. Duchêne and J. Thibonnet, *J. Organomet. Chem.*, 2005, **690**, 4835–4843.

14 (*a*) P. Lu, T. C. Boorman, A. M. Z. Slawin and I. Larrosa, *J. Am. Chem. Soc.*, 2010, **132**, 5580–5581; (*b*) X. C. Cambeiro, N. Ahlsten and I. Larrosa, *J. Am. Chem. Soc.*, 2015, **137**, 15636–15639.

15 S. C. F. Kui, J.-S. Huang, R. W.-Y. Sun, N. Zhu and C.-M. Che, *Angew. Chem. Int. Ed.*, 2006, **45**, 4663–4666.

16 (*a*) M. C. Gimeno, J. Jiménez, P. G. Jones, A. Laguna and M. Laguna, *Organomet.*, 1994, **13**, 2508–2511; (*b*) A. Laguna, M. Laguna, J. Jiménez, F. J. Lahoz, E. Olmos, *Organomet.*, 1994, **13**, 253–257; (*c*) R. Usón, A. Laguna, M. Laguna, J. Jiménez, P. G. Jones, *Angew. Chem. Int. Ed.*, 1991, **30**, 198–199.

17 J. Mei, N. L. C. Leung, R. T. K. Kwok, J. W. Y. Lam and B. Z. Tang, *Chem. Rev.*, 2015, **115**, 11718–11940.

18 (*a*) W. Lu, K. T. Chan, S.-X. Wu, Y. Chen and C.-M. Che, *Chem. Sci.*, 2012, 3, 752-755; (*b*) G. S. M. Tong, K. T. Chan, X. Chang and C.-M. Che, *Chem. Sci.*, 2015, 6, 3026-3037; (*c*) G. Chakkaradhari, Y.-T. Chen, A. J. Karttunen, M. T. Dau, J. Jänis, S. P. Tunik, P.-T. Chou, M.-L. Ho and I. O. Koshevoy, *Inorg. Chem.*, 2016, **55**, 2174–2184.